Predicting structure and property relations in polymeric photovoltaic devices

Gavin A. Buxton and Nigel Clarke
Department of Chemistry, University of Durham, Durham, DH1 3LE, United Kingdom
(Received 16 December 2005; published 18 August 2006)

Plastic solar cells are attractive candidates for providing cheap, clean, and renewable energy. However, such devices are critically dependent on the internal structure, or morphology, of the polymer constituents. We have developed a model that enables us to predict photovoltaic behavior for arbitrary morphologies, which we also generate from numerical simulations. We illustrate the model by showing how diblock copolymer morphologies can be manipulated to optimize the photovoltaic effect in plastic solar cells. In this manner, we can correlate photovoltaic properties with device structure and hence guide experiments to optimize polymer morphologies to meet photovoltaic needs.

DOI: 10.1103/PhysRevB.74.085207 PACS number(s): 72.20.Ee, 72.20.Jv, 72.80.Le

The use of polluting fossil fuels, and the greenhouse gases they produce, is believed to have made a devastating impact on our environment. Ice sheet disintegration, sea level rise, and other long-term detrimental effects have driven research into finding alternative energy sources.[1] A promising route to producing clean and renewable energy is through the use of solar cells, which harvest power directly from sunlight. In particular, plastic solar cells open up the possibility of fabricating inexpensive large-area devices at relatively low temperatures.[2] Furthermore, plastic devices can be mechanically flexible, processed into complex shapes, and colored depending upon their chemical structure, leading the way to new and more interesting photovoltaic applications.[2] Computational studies can offer materials scientists a unique insight into the mechanics of these polymer solar cells and, in particular, the role polymer blend morphologies play in device performance. We show how computer simulations can be used to not only predict polymer morphologies, but how the output from our morphological studies can be used as the input to a computer model of photovoltaic behavior. Therefore, we can correlate polymer structure and photovoltaic properties, showing how choices made regarding the polymeric constituents and processing conditions can ultimately affect the solar cell performance.

Typically, an organic solar cell consists of two distinct materials sandwiched in between two electrodes of differing work functions (resulting in an internal electric field). One material is hole transporting while the other is electron transporting (often referred to as donor and acceptor materials). Either material is capable of absorbing a photon, resulting in the formation of an electron-hole pair, the electron and hole being bound to each other by their electrostatic attraction (see Fig. 1). This bound pair constitutes an "exciton" and can be thought of as a mobile excited state.[3] Excitons are strongly bound in organic materials but may dissociate at the interface between two materials with different electron affinities and ionization potentials.[4] Once the charge carriers are dissociated at the donor-acceptor (DA) interface the internal electric field sweeps electrons to the cathode and holes to the anode, thus allowing this current to be used in the external circuit.

Exciton dissociation depends critically on the DA interface; hence, the performance of organic solar cells is highly sensitive to the morphology. Excitons generally diffuse ~10 nm prior to decay and must reach an interface within this distance in order for dissociation to occur. Meanwhile, high absorption coefficients in organic materials lead to 100 nm, or thicker, devices. It is this difference in length scales, and the need to ensure charge transport from the DA interface to the electrodes, which results in devices which are very sensitive to morphological effects.[5]

The simplest organic photovoltaic cell is the bilayer device originally proposed by Tang.[4] After exciton dissociation electrons are found in the acceptor and holes in the donor, resulting in large asymmetric charge-carrier gradients at the interface. This means that not only is current conveyed to the circuit because of the internal electric field, but also because of a diffusion current.[3,6] However, as only the excitons generated within ~10 nm of the DA interface have a chance to dissociate, most excitons decay prior to dissociation, wasting absorbed solar energy.

In order to overcome this loss mechanism a morphology whose domain size is comparable to the exciton diffusion length is required. Bulk heterojunction devices, comprised of bicontinuous and interpenetrating networks of donor and ac-

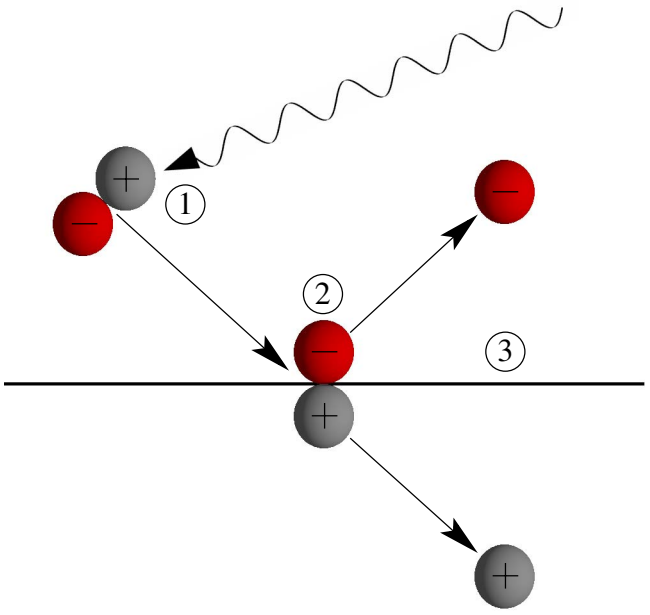

FIG. 1. (Color online) Illustration of (1) photon absorption, (2) exciton dissociation, and (3) charge transport.

ceptor materials, satisfy this requirement.[7–9] Blending the donor and acceptor polymers, such that no point is more than a few nanometers from a DA interface, results in efficient charge generation throughout the whole volume of the device. However, this convoluted morphology possesses resistive bottlenecks and cul-de-sacs which prohibit free charges from reaching the electrodes.

In order to ensure efficient charge carrier transport an idealized morphology must be realized. Coakley *et al.*[10,11] produced an ideal device architecture for organic-inorganic solar cells. The morphology consisted of straight phases aligned perpendicular to the substrate, but with only the appropriate phase being connected to the electrodes. Not only are excitons generated close to a DA interface, but there are also uninterrupted pathways to the electrodes. The phases are connected exclusively to the appropriate electrodes to ensure that only electrons diffuse in the desired direction to the electron-withdrawing electrode and, likewise, only holes diffuse to the hole-withdrawing electrode. Therefore, the charge carriers drift towards their respective electrodes due to the built-in electric field and also diffuse towards the electrodes based entirely on the internal morphology of the device. Coakley *et al.*[10,11] produced devices that were *3 times* more efficient than equivalent planar devices.

Recently, there has been a flurry of interest in semiconducting diblock copolymers.[12–14] The intrinsic length scale of phase separation in diblock copolymers makes them ideal constituents for organic solar cells. Furthermore, the morphology of diblock copolymer systems can be manipulated. For example, surface-induced ordering of diblock copolymers can lead to domains oriented either parallel or perpendicular to the surface.[15] Diblock copolymer domains can also be aligned through the application of an electric field.[16] What we propose here is a method of controlling the phase separation dynamics of diblock copolymers in order to produce ideal morphologies for photovoltaic applications.

In order to predict the morphologies in these systems we employ the Flory-Huggins Cahn-Hilliard model, where the free energy is of the form

$$F = \int \frac{1}{N}\{\phi(\mathbf{r})\ln\phi(\mathbf{r}) + [1-\phi(\mathbf{r})]\ln[1-\phi(\mathbf{r})]\} + \chi\phi(\mathbf{r})[1-\phi(\mathbf{r})] + \frac{b^2|\nabla\phi(\mathbf{r})|^2}{36\phi(\mathbf{r})[1-\phi(\mathbf{r})]}d\mathbf{r} + \frac{\alpha}{2}\int\int G(\mathbf{r},\hat{\mathbf{r}})[\phi(\mathbf{r})-\bar{\phi}][\phi(\hat{\mathbf{r}})-\bar{\phi}]d\mathbf{r}d\mathbf{r}' + \int -\frac{\epsilon(\phi)|\mathbf{E}|^2}{8\pi}d\mathbf{r} + \int\int \frac{1}{2}V\exp(-|\mathbf{r}-\mathbf{s}|/r_0) \times[\phi(\mathbf{r})-\phi_S]^2 d\mathbf{r}d\mathbf{s}, \quad (1)$$

where $\phi(\mathbf{r})$ is the local concentration of donor polymers. The first two terms are the usual Flory-Huggins terms, where N is the degree of polymerization and χ is the enthalpic interaction parameter.[17] The third term energetically penalizes concentration gradients and drives domain coarsening. The fourth term is a long-range interaction which accounts for the connectivity of diblock copolymers, where $G(\mathbf{r},\mathbf{r}')$ is defined by $-\nabla^2 G(\mathbf{r},\mathbf{r}') = \delta(\mathbf{r}-\mathbf{r}')$.[18] The fifth term represents the electrostatic free energy of a material of dielectric constant ϵ in an electric field $\mathbf{E}$.[19] Finally, the last term represents the interaction of a fluid at $\mathbf{r}$ with a surface $\mathbf{s}$, which is either preferential to donor ($\phi_S=1$) or acceptor ($\phi_S=0$) material.[20] The kinetic equation (of the form $\partial\phi/\partial t = \nabla\cdot M\nabla[\partial F/\partial\phi]$) can be discretized and solved numerically using the finite-difference technique.[21]

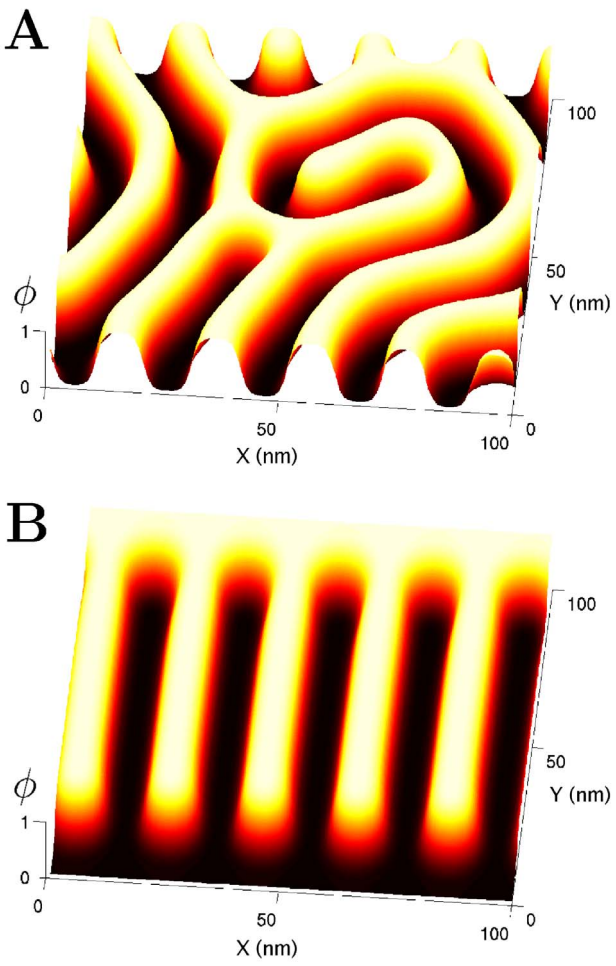

FIG. 2. (Color online) Diblock copolymer thin film morphologies showing (a) disordered and (b) ideal structures. The parameters governing the diblock copolymer are $N=10\,000$, $\chi=0.015$, $b=0.24$ nm, and $\alpha=0.001$. The ideal morphology was created by introducing a range of interaction, $r_0=3$ nm, at the surface and an electric field of $E=3.5\times10^5$ V m^{-1}. The dielectric constants of the donor and acceptor are 3 and 4, respectively.

Figure 2(a) depicts a snapshot of a diblock copolymer phase separating in the absence of an electric field, with periodic and no-flux boundary conditions in the x and y directions, respectively. While the morphology is bicontinuous, it is also tortuous and disordered. However, order can be imposed. The upper surface can be made to be preferential to donor polymers and the lower surface to acceptor polymers. Furthermore, an electric field can be applied in the y direction, resulting in the morphology depicted in Fig. 2(b). This morphology is ideal for organic solar cells in that the DA

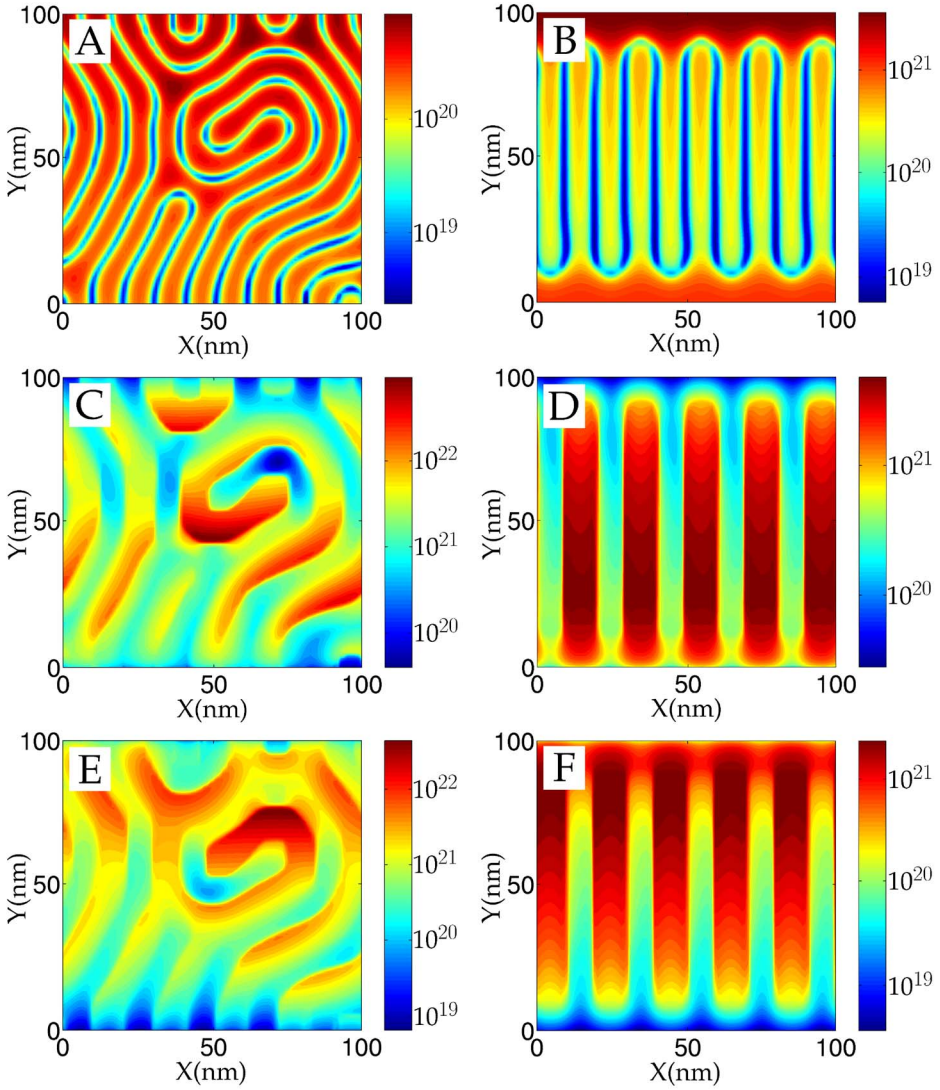

FIG. 3. (Color online) Concentration profiles for excitons [(a) and (b)], electrons [(c) and (d)], and holes [(e) and (f)]. Systems with both disordered [(a), (c), and (e)] and ideal [(b), (d), (f)] morphologies are depicted. The mobilities of electrons in the acceptor and donor are 1×10^{-8} and 1×10^{-9} $m^2\,V^{-1}\,s^{-1}$, respectively. The mobilities of holes in the acceptor and donor are 2×10^{-9} and 2×10^{-8} $m^2\,V^{-1}\,s^{-1}$, respectively. The exciton mobility $\mu_x=3.86\times10^{-9}$ $m^2\,V^{-1}\,s^{-1}$ takes into account a diffusion length of 10 nm and a lifetime τ_x of 1×10^{-6} s. The field-dependent mobility parameter is $\gamma=5\times10^{-4}$ $m^{1/2}\,V^{-1/2}$. The polaron binding energy is $E_p=0.1$ eV, the band offset between donor and acceptor is $\Delta E=0.7$ eV, the exciton binding energy is 0.5 eV, and the Schottky barrier height is 0.5 eV. The built-in voltage is 0.5 V.

domains are orientated perpendicular to the electrodes, while at the same time the donor and acceptor material is exclusively in contact with the anode and cathode, respectively.

We can now simulate the photovoltaic response of devices which possess these *exact* morphologies. Thereby, we not only elucidate the physical mechanisms governing the operation of organic solar cells, but also correlate photovoltaic properties with device structure. It should also be noted that we do not limit our investigation to any particular system, but choose typical material parameters in order to capture the general physics of these devices. To simulate these systems, we utilize the drift-diffusion method,[6,22] which involves finding the self-consistent solution of the following equations for the electrostatic potential (ψ) and the electron (n), hole (p), and exciton (x) densities:

$$\nabla\cdot(\epsilon\nabla\psi) = -q(p-n),$$

$$\frac{\partial n}{\partial t} = D(\mathbf{E}) - R(n,p) - \frac{1}{q}\nabla[qn\mu_n\nabla\psi - k_\beta T\mu_n\nabla n],$$

$$\frac{\partial p}{\partial t} = D(\mathbf{E}) - R(n,p) - \frac{1}{q}\nabla[-qp\mu_p\nabla\psi - k_\beta T\mu_p\nabla p],$$

$$\frac{\partial x}{\partial t} = G(\mathbf{r}) + \frac{1}{4}R(n,p) - R(x) - D(\mathbf{E}) - \frac{1}{q}\nabla[-k_\beta T\mu_x\nabla x]. \tag{2}$$

Solving these equations allows us to obtain the local densities and current distributions, along with the global *I-V*

curves, given the initial device morphology and material parameters.[6,22] The photogeneration of excitons is given by $G(\mathbf{r})=\Sigma_i \Phi_i(r_x)\alpha_i \exp^{-\alpha_i(L_y-r_y)}$, where $\Phi_i(r_x)$ is the incident photon flux[23] and α_i is the absorption coefficient (taken to be a Gaussian distribution with an average of 500 nm, standard deviation of 75 nm, and maximum peak of 2×10^5 cm^{-1}). Exciton dissociation is described by Onsager's theory for electrolytic dissociation and given by $D(\mathbf{E})=N_f\int_0^\infty k_D(\mathbf{E},a)F(a)da$, where $k_D(\mathbf{E},a)$ is the electric-field-dependent rate constant given by Braun.[24] We take the electric field to be due to both local variations in electrostatic potential and regional differences in electron affinity and ionization potential.[5] Because of the local disorder in polymeric materials, the dissociation rate is integrated over a Gaussian distribution of separation distances a. $F(a)$ represents this distribution function, and N_f is a normalization factor. $R(x)=x/\tau_x$ represents exciton decay, where τ_x is the average lifetime of an exciton. Free charge carriers recombine with a recombination rate of the Langevin form, $R(n,p)=q(\mu_n+\mu_p)pn/\epsilon$. A fraction (commonly taken as $\frac{1}{4}$) recombine to form excitons. Current transport in organic semiconductors is a hopping process which can be phenomenologically captured with a field-dependent carrier mobility of the familiar Poole-Frenkel form $\mu=\mu_0\exp(\gamma\sqrt{|\mathbf{E}|})$.

We adopt the strategy of Ruhstaller *et al.*[25] for simulating the hopping process at internal interfaces. They assumed that the hopping rate between two sites differing in energy by ΔE is proportional to $\exp[-(\Delta E+E_p)^2/4kTE_p]$, where E_p is the polaron binding energy. For metal-semiconductor interfaces we adopt the boundary conditions of Scott and Malliaras.[26] The precise form of the current in these Schottky barriers can be found in Barker *et al.*[6] The Scharfetter-Gummel method[27] is used to spatially discretize the above equations, which are solved semi-implicitly using the finite-difference method.[22] In this manner, the physics of organic solar cells can be captured.

It is worth noting that while commercially available drift-diffusion models can simulate inorganic devices they do not currently account for the generation, diffusion, or dissociation of excitons in organic devices. Previous studies that have computationally investigated organic solar cells have either neglected excitons altogether[3] (assuming that electrons and holes are simply "generated" at the interface) or been limited to bilayer devices.[6] Here, we simulate the diffusion of electrons, holes, and excitons throughout the system which enables us to simulate the effects of complex internal morphologies.

Contour plots of exciton density are shown in Figs. 3(a) and 3(b), corresponding to the disordered and ideal morphologies. In both systems the morphology is clearly evident as exciton dissociation occurs almost exclusively at the DA interface. Excitons are diffusing to the DA interface where they are most likely to dissociate. The electron and hole concentrations are also depicted in Figs. 3(c)–3(f). The internal electric field is such that it sweeps electrons to the cathode ($y=0$) and holes to the anode ($y=100$). However, in the convoluted disordered system the electrons and holes are prohibited from reaching the electrodes by the presence of "dead ends" in the morphology. In other words, the charge carriers travel down cul-de-sacs only to find themselves surrounded by the DA interface. This results in large charge-carrier concentrations at dead ends, such that the diffusion process away from a dead end opposes the drift process due to the internal electric field. However, in the ideal morphology it can be seen that the charge carriers have a direct pathway from the DA interface to the correct electrodes. Therefore, not only are excitons efficiently dissociated, but the charge carriers are easily swept to the electrodes by the internal electric field.

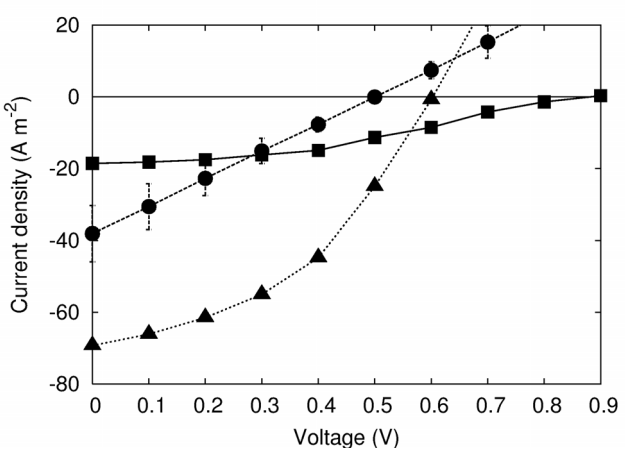

FIG. 4. Current-voltage (I-V) curves for systems with planar (■), disordered bulk heterojunction (•), and ideal (▲) morphologies. I_{sc} is defined as the current when $V=0$ and, similarly, V_{oc} is defined as the applied voltage when $I=0$. The power conversion efficiency is given by the maximum value of I-V divided by the total solar irradiance.

The effects of this on the I-V curves can be seen in Fig. 4 which depicts the response of systems with bilayer, bulk heterojunction, and ideal morphologies. The planar device has little short-circuit current (I_{sc}), due to fewer charge carriers being present. However, the open-circuit voltage (V_{oc}) is large as a consequence of the large diffusion currents in these systems.[3,6] The bulk heterojunction has a V_{oc} due entirely to the difference in work function between the two electrode metals (~0.5 V). This is because in this symmetric system there is no net diffusion process. I_{sc} is greater in the bulk heterojunction than in the planar device as the larger interfacial area results in a greater charge carrier generation. This is also the case for the ideal morphology, except now the charge carriers can drift to the correct electrodes unimpeded and, hence, the I_{sc} is much greater in these systems. The planar device has a power conversion efficiency of ~0.7% which is reasonable for such systems.[4] The bulk heterojunction systems, for the parameters considered here, actually perform slightly worse than the planar device and possess efficiencies of ~0.6%. However, the devices with an ideal morphology have a much higher efficiency of ~2.2%: *3 times* greater than the planar device. This highlights the role of morphology in these systems and emphasizes the superiority of the ideal morphology over both the planar and disordered bulk heterojunction morphologies.

To summarize, we have simulated the photovoltaic mechanism in organic solar cells and elucidated exciton

diffusion, exciton dissociation, and charge transport processes in these devices. Furthermore, we have investigated the effects of complex diblock copolymer morphologies on device performance and, in particular, tailored these morphologies to meet photovoltaic needs. We have shown how surface-induced ordering and electric-field-induced alignment can be combined to create ideal morphologies for photovoltaic applications.

[1] J. Hansen, L. Nazarenko, R. Ruedy, M. Sato, J. Willis, A. Del Genio, D. Koch, A. Lacis, K. Lo, S. Menon, T. Novakov, J. Perlwitz, G. Russel, G. A. Schmidt, and N. Tausnev, Science **308**, 1434 (2005).

[2] S. E. Shaheen, D. S. Ginley, and G. E. Jabbour, MRS Bull. **30**, 10 (2005).

[3] B. A. Gregg and M. C. Hanna, J. Appl. Phys. **93**, 3605 (2003).

[4] C. W. Tang, Appl. Phys. Lett. **48**, 183 (1986).

[5] J. Nelson, Science **293**, 1059 (2001).

[6] J. A. Barker, C. M. Ramsdale, and N. C. Greenham, Phys. Rev. B **67**, 075205 (2003).

[7] G. Yu and A. J. Heeger, J. Appl. Phys. **78**, 4510 (1995).

[8] G. Yu, J. Gao, J. C Hummelen, F. Wudl, and A. J. Heeger, Science **270**, 1789 (1995).

[9] J. J. M. Halls, C. A. Walsh, N. C. Greenham, E. A. Marseglia, R. H. Friend, S. C. Moratti, and A. B. Holmes, Nature (London) **376**, 498 (1995).

[10] K. M. Coakley and M. D. McGehee, Appl. Phys. Lett. **83**, 3380 (2003).

[11] K. M. Coakley, Y. Liu, C. Goh, and M. D. McGehee, MRS Bull. **30**, 37 (2005).

[12] U. Stalmach, B. de Boer, C. Videlot, P. F. van Hutten, and G. Hadziioannou, J. Am. Chem. Soc. **122**, 5464 (2000).

[13] B. de Boer, U. Stalmach, P. F. van Hutten, C. Melzer, V. V. Krasnikov, and G. Hadziioannou, Polymer **42**, 9097 (2001).

[14] S. M. Lindner and M. Thelakkat, Macromolecules **37**, 8832 (2004).

[15] T. Xu, C. J. Hawker, and T. P. Russell, Macromolecules **38**, 2802 (2005).

[16] T. L. Morkved, M. Lu, A. M. Urbas, E. E. Ehrichs, H. M. Jaeger, P. Mansky, and T. P. Russell, Science **273**, 931 (1996).

[17] P. J. Flory, *Principles of Polymer Chemistry* (Cornell University Press, Ithaca, NY, 1953).

[18] T. Ohta and K. Kawasaki, Macromolecules **19**, 2621 (1986).

[19] L. D. Landau and E. M. Lifshitz, *Electrodynamics of Continuous Media* (Pergamon Press, Oxford, 1960).

[20] O. Kuksenok, D. Jasnow, J. Yeomans, and A. C. Balazs, Phys. Rev. Lett. **91**, 108303 (2003).

[21] S. C. Glotzer, Annu. Rev. Comput. Phys. **2**, 1 (1995).

[22] S. Selberherr, *Analysis and Simulation of Semiconductor Devices* (Springer-Verlag, Wien, 1984).

[23] We take the air-mass 1.5 solar data from A. L. Fahrenbruch and R. H. Bube, *Fundamental of Solar Cells* (Academic Press, New York, 1983). The total irradiance is 831.8 W m^{-2}.

[24] C. L. Braun, J. Chem. Phys. **80**, 4157 (1984).

[25] B. Ruhstaller, S. A. Carter, S. Barth, H. Riel, W. Riess, and J. C. Scott, J. Appl. Phys. **89**, 4575 (2001).

[26] J. C. Scott and G. G. Malliaras, Chem. Phys. Lett. **299**, 115 (1999).

[27] D. L. Scarfetter and H. K. Gummel, IEEE Trans. Electron Devices **16**, 64 (1969).